

Generating 3D Adversarial Point Clouds

Chong Xiang

Shanghai Jiao Tong University
Shanghai, China
xiangchong97@gmail.com

Charles R. Qi

Stanford University
California, USA
charlesq34@gmail.com

Bo Li

University of Illinois at Urbana-Champaign
Illinois, USA
lxbosky@gmail.com

Abstract

Machine learning models especially deep neural networks (DNNs) have been successfully applied to a variety of applications. However, DNNs are known to be vulnerable to adversarial examples which are carefully crafted instances aiming to cause learning models to make incorrect predictions. Recently, adversarial examples have been extensively studied for 2D image, natural language and audio datasets, while the robustness of 3D models has not yet been explored. Given the wide safety-critical applications of 3D models, such as PointNet for Lidar data in autonomous driving, it is important to understand the vulnerability of 3D models under various adversarial attacks. Due to the special format of point cloud data compared with 2D images, it is challenging to generate adversarial examples directly in the point cloud space. In this work, we propose several novel algorithms to generate adversarial point clouds against PointNet, which is the most widely used model dealing with light-weight but irregularly formatted point cloud data. We mainly propose two types of attacks on point clouds: unnoticeable adversarial point clouds, and manufacturable adversarial point clusters for physical attacks. For unnoticeable point clouds, we propose to either shift existing or add new points negligibly to craft “unnoticeable” perturbation. For adversarial point clusters, we propose to generate a small number (1-3) of explicit “manufacturable adversarial point clusters” which are noticeable but of meaningful clusters. The goal of these adversarial point clusters is to realize “physical attacks” by 3D printing the synthesized objects and sticking them to the original object. In addition, we propose 7 perturbation measurement metrics tailored to different attacks and conduct extensive experiments to evaluate the proposed algorithms on the ModelNet40 dataset. Overall, our attack algorithms achieve about 100% attack success rate for all targeted attacks¹.

Introduction

Despite of the great success in various learning tasks, deep neural networks (DNNs) have been found vulnerable to adversarial examples. The adversary is able to add imperceptible perturbation to the original data and mislead DNNs with high confidence. Many algorithms have been proposed to generate adversarial examples for data such as 2D images (Szegedy et al. 2013; Goodfellow, Shlens,

and Szegedy 2014; Papernot et al. 2016; Moosavi-Dezfooli, Fawzi, and Frossard 2016; Carlini and Wagner 2017), natural languages (Jia and Liang 2017; Zhao, Dua, and Singh 2017), and audios (Carlini and Wagner 2018; Das et al. 2018). Several recent works (Athalye and Sutskever 2017; Evtimov et al. 2017) have proposed adversarial examples in the physical world, but they simply project 3D real-world objects to 2D images as data pre-processing. No existing work has explored the vulnerability of actual 3D models. In this paper, we study the robustness of 3D models which directly deal with 3D objects instead of projecting the object to 2D. Specifically, we choose 3D point cloud data and the commonly used PointNet model (Qi et al. 2016) and its variations as our targets.

A point cloud is an importance geometric data structure which has the advantage of flexible representation and low storage requirement. After the notorious problem of irregular data format was addressed by PointNet (Qi et al. 2016) and its variants (Qi et al. 2017; Wang et al. 2018), point cloud data is able to be directly processed by DNNs, and has become a promising data structure for 3D computer vision tasks. Since techniques like Lidar has been widely deployed in safety-critical scenarios such as autonomous driving (Zermas, Izzat, and Papanikolopoulos 2017), the robustness of 3D point cloud models against adversarial examples is of great importance. Given the special properties of point cloud 3D data, generating adversarial point clouds is challenging. Point cloud’s irregular data format has made existing attack algorithms designed for 2D instances unusable: 1) There is no “pixel values” positioned in the fixed dimensions that could be slightly modified, so new attack strategies are required; 2) The unconstrained data space (points can be added to arbitrary positions) results in extremely large searching space; 3) The commonly used L_p norm measurement in 2D images to bound the perturbation does not work for such changeable data dimensionality in 3D.

To the best of our knowledge, we are the first to extend adversarial example research to irregular point cloud data and provide solutions to aforementioned challenges. We propose several novel attack methods for mainly two types of adversarial attacks on point cloud data: *unnoticeable adversarial point clouds*, and *manufacturable adversarial point clusters* for physical attacks. For unnoticeable adversarial point clouds, we propose to either shift existing or add new

¹Untargeted attacks are easier to achieve with the proposed methods, so in this paper we only focus on targeted attacks.

points negligibly, bounded by different perturbation metrics. To measure the attack performance, we propose to use L_2 norm, Hausdorff Distance, Chamfer Measurement, and the number of added points as perturbation metrics. Our experiments show that we are able to craft unnoticeable adversarial point clouds with 100% success rate given an acceptable perturbation budget.

While the unnoticeable adversarial point clouds require to manipulate 3D points over different positions on the surface which is hard to realize in the physical world, we also propose to synthesize and attach *manufacturable adversarial point clusters* to original objects. In particular, we search for vulnerable regions of objects, initialize adversarial clusters, and optimize the positions and shapes of clusters. Such generated adversarial points clusters can be manufactured via 3D printing, and attached to the original objects to mount physical attacks. We leverage both farthest distance loss and center loss to constrain and evaluate the size of each cluster. The number of added clusters is also considered in evaluation. Our attack achieves 99.9% attack success rate when adding 3 adversarial clusters, 99.6% with two, and 84.2% with one. In addition, we evaluate the transferability of our generated adversarial point clouds among different 3D models including PointNet++ (Qi et al. 2017) and DGCNN (Wang et al. 2018). Our initial observation is that such 3D adversarial point clouds are harder to transfer compared with 2D images, which provides possibility for black-box defense against 3D adversarial instances.

Overall, the contributions of this paper can be summarized as follows:

- We are the first to generate 3D adversarial point clouds against 3D learning models and provide baseline evaluations for future research.
- We demonstrate unique challenges in dealing with irregular data structures such as point clouds and provide several solutions towards them.
- We propose novel algorithms to both craft *unnoticeable adversarial point clouds* by either shifting existing or adding new points, and generate *manufacturable adversarial point clusters* for physical attacks.
- We propose 7 different perturbation metrics tailored to different attack tasks.
- We perform extensive experiments and show our attack algorithms can achieve about 100% attack success rate for all targeted attacks.
- We provide transferability analysis for 3D point cloud data and show that analyzing properties of different 3D models sheds light on potential defenses for 2D instances.

Related Work

Point Clouds and PointNet. The point cloud data is notorious for its unordered and dimensionality-flexible data format which thwarts direct learning from the data via traditional neural networks. In order to address this problem, PointNet (Qi et al. 2016) is proposed and widely used for

direct point cloud data processing. PointNet and its variants (Qi et al. 2017; Wang et al. 2018) exploit a single symmetric function, *max pooling*, to reduce the unordered and dimensionality-flexible input data to a fixed-length global feature vector and enable end-to-end neural network learning. Qi et al. also tried to demonstrate the robustness of the proposed PointNet and introduced the concept of critical points and upper bounds. They showed that points sets laying between critical points and upper bounds yield the same global features and thus PointNet is robust to missing points and random perturbation. However, they did not study the robustness of PointNet against adversarial manipulations, which is the main focus of this paper.

Adversarial Examples. Szegedy et al. (Szegedy et al. 2013) first pointed out that machine learning models such as neural networks were vulnerable to carefully crafted adversarial perturbation. An adversarial example which appears similar to its original data can easily fool the neural networks with high confidence. Such vulnerability of machine learning models has raised great concerns in the community and many works have been proposed to improve the attack performance (Goodfellow, Shlens, and Szegedy 2014; Papernot et al. 2016; Moosavi-Dezfooli, Fawzi, and Frossard 2016; Carlini and Wagner 2017; Papernot et al. 2017; Xiao et al. 2018b; Xiao et al. 2018a) and search for possible defense (Carlini and Wagner 2016; Meng and Chen 2017; Xu, Evans, and Qi 2017; Ranjan et al. 2017; Samangouei, Kabkab, and Chellappa 2018; Yan, Guo, and Zhang 2018). The state-of-the-art attack algorithm, optimization based attack (Carlini and Wagner 2017), defines an objective loss function which measures both attack effectiveness and perturbation magnitude, and uses optimization to find a near-optimal adversarial solution. However, the algorithm only deals with 2D data. Several recent works (Kurakin, Goodfellow, and Bengio 2016; Athalye and Sutskever 2017; Evtimov et al. 2017) also study the adversarial examples in the physical world. Athalye and Sutskever manage to create adversarial examples robust to camera viewpoint changes. Evtimov et al. try to fool traffic sign detection system in autonomous vehicles. However, these works only project physical objects to 2D images and do not study models which directly deal with 3D objects. To the best of our knowledge, we are the first to generate adversarial examples for 3D machine learning models.

Problem Statement

Point Cloud Data. A point cloud is a set of points which are sampled from object surfaces. A data record $x \in \mathbb{R}^{n \times 3}$ corresponds to a point set of size n , where each point is represented by a 3-tuple (x, y, z) coordinate. One most important characteristic of point cloud data is its flexible dimensionality ($n \times 3$). This flexibility, however, brings fatal problems for existing attack algorithms and perturbation metrics, since they are designed for fixed-shape data only. Moreover, we are able to add points at any positions in the 3D space, and such lack of constrain results in an extremely large search space for adversarial examples. New attack algorithms should be proposed to address the problems of flexible dimensionality and large search space.

Targeted Adversarial Attacks. In this paper, we only focus on targeted attacks against 3D point cloud classification models. It is flexible to extend our algorithms to other tasks like attacking segmentation models. The goal of targeted attacks is to mislead the PointNet model to classify an adversarial example as a selected target class with smallest perturbation. In this paper, we consider two kinds of point cloud *perturbation*, namely point shifting and point adding². Formally, for a classification model $\mathcal{F} : \mathcal{X} \rightarrow \mathcal{Y}$, which maps an input $x \in \mathcal{X} \subset \mathbb{R}^{n \times 3}$ to its corresponding class label $y \in \mathcal{Y} \subset \mathbb{Z}$, an adversary has a malicious target class $t' \in \mathcal{Y}$. Based on a perturbation metric $\mathcal{D} : \mathbb{R}^{n \times 3} \times \mathbb{R}^{n' \times 3} \rightarrow \mathbb{R}$, the goal of the attack is to find a legitimate input $x' \subset \mathbb{R}^{n' \times 3}$ which:

$$\min \mathcal{D}(x, x'), \quad s.t. \mathcal{F}(x') = t' \quad (1)$$

Note that, for point cloud data, n is not necessarily equal to n' .

As mentioned in (Carlini and Wagner 2017), directly solving this problem is difficult. Therefore, we reformulate the problem as gradient-based optimization algorithms:

$$\min f(x') + \lambda * \mathcal{D}(x, x') \quad (2)$$

Here $f(x') = (\max_{i \neq t'} (\mathcal{Z}(x')_i) - \mathcal{Z}(x')_{t'})^+$ is the adversarial loss function whose output measures the possibility of an successful attack, where $\mathcal{Z}(x)_i$ is the i^{th} element of the logits vector and $(r)^+$ represents $\max(r, 0)$. By optimizing over Equation 2, we aim to search for adversarial examples by adding negligible 3D perturbation.

3D Unnoticeable and Manufacturable Adversarial Perturbation. In this paper, we consider two different attack scenarios. Firstly, we propose to craft *unnoticeable adversarial point clouds*. We assume the adversary is able to arbitrarily perturb (i.e., shift or add) points which are directly fed to the PointNet model. Secondly, we propose to generate *manufacturable adversarial point clusters* for physical attacks. The adversary for this attack is able to stick manufacturable (i.e., able to be 3D printed) point clusters to the original objects. In the following two sections, we will introduce our proposed algorithms for these two attacks.

3D Unnoticeable Adversarial Point Clouds

In this section, we focus on generating unnoticeable adversarial point clouds. We first introduce perturbation evaluation metrics \mathcal{D} tailored to point cloud data, and then explain how to generate unnoticeable adversarial point clouds by shifting existing and adding new points. Note that when adding new points to the original point clouds, we have to deal with data dimensionality changes.

Perturbation Metrics

For point clouds, the perturbation metrics should not have assumption on the stability of data dimensionality, except in

²To guarantee the points can still cover the whole surface of an object, we will not allow an adversary to remove points.

one special case when we only shift existing points. Therefore, we choose L_p norm and other two point set based distances as our metrics.

L_p Norm. The L_p norm is a commonly used metric for adversarial perturbation of fixed-shape data. For the original point sets \mathcal{S} and corresponding adversarial set \mathcal{S}' , the L_p norm of the perturbation is defined as:

$$\mathcal{D}_{L_p} = \left(\sum_i (\mathcal{S}_i - \mathcal{S}'_i)^p \right)^{\frac{1}{p}} \quad (3)$$

where \mathcal{S}_i is the i^{th} point coordinate in set \mathcal{S} , and \mathcal{S}'_i is its corresponding point in set \mathcal{S}' . Note that in our attack, L_p norm can only be used when we are crafting adversarial point clouds by shifting existing points. Specifically, we choose L_2 norm for our attack.

Hausdorff Distance. Hausdorff distance is often used to measure how far two subsets of a metric space are from each other. Formally, for an original point set \mathcal{S} and its adversarial counterpart \mathcal{S}' , the Hausdorff distance is defined as:

$$\mathcal{D}_H(\mathcal{S}, \mathcal{S}') = \max_{y \in \mathcal{S}'} \min_{x \in \mathcal{S}} \|x - y\|_2^2 \quad (4)$$

Intuitively, Hausdorff distance finds the nearest original point for each adversarial point and outputs the maximum square distance among all such nearest point pairs.

Chamfer Measurement.³ Chamfer measurement (Fan, Su, and Guibas 2017) is a similar perturbation metric as Hausdorff distance. The difference is Chamfer distance takes the average, rather than the maximum, of all nearest point pairs. The formal definition is as follows:

$$\mathcal{D}_C(\mathcal{S}, \mathcal{S}') = \frac{1}{\|\mathcal{S}'\|_0} \sum_{y \in \mathcal{S}'} \min_{x \in \mathcal{S}} \|x - y\|_2^2 \quad (5)$$

Number of Points Added. We also want to measure the number of points added in our attack. Since points shifted or added to the object surface in our attack do not change the shape of object, we will only count the points whose distance from surface is above a certain threshold. Formally, for a original point set \mathcal{S} , the generated point set \mathcal{S}' , and a threshold value T_{thre} , the number of points added is defined as:

$$Count(\mathcal{S}, \mathcal{S}') = \sum_{y \in \mathcal{S}'} \mathbb{1}[\min_{x \in \mathcal{S}} \|x - y\|_2 > T_{thre}] \quad (6)$$

where $\mathbb{1}[\cdot]$ is the indicator function whose value is 1 when the statement is true and 0 otherwise. Note that the number of points added is not optimized as the perturbation metric \mathcal{D} in Equation 2 due to its incompatibility with gradient-based optimization algorithms, but is reported as an additional performance metric.

Generating Unnoticeable Point Clouds

After choosing the appropriate perturbation metric \mathcal{D} , we are able to take advantage of Equation 2 and generate unnoticeable adversarial point clouds with near-optimal perturbation.

³We name it as ‘‘Chamfer measurement’’ since this perturbation metric does not satisfy triangle inequality, which means it does not satisfy the definition of distance.

Shifting Existing Points. Since the dimensionality of the original point cloud and the shifted point cloud are equal, we can optimize directly over Equation 2. Here we choose L_2 norm distance as the distance function to bound the shifting perturbation.

Adding Adversarial Points. Directly adding points to the unconstrained 3D space is infeasible due to the large search space. Therefore we propose an *initialize-and-shift* method to find appropriate position for each added point:

1. *Initialize* a number of points to the same coordinates of existing points as initial points.
2. *Shift* initial points via optimizing Equation 2 and output their final positions.

Since PointNet uses the max pooling to learn the global features, the initial points sharing the same positions with original points do not change the output of PointNet model. In other words, the point cloud composed of original points and initial points is still a benign example. During the optimization process, some initial points are shifted from their initial positions and “added” to the original objects as adversarial points. The other initial points which are barely shifted and remain on the surface of the object do not change the shape of the object, and thus can be discarded by Equation 6 as points-not-added. This is another advantage of *initialize-and-shift* method: we do not need to fine-tune the number of initial points. As long as we add proper perturbation constraints, we can generate good adversarial examples and discard points which are not counted by Equation 6.

One last question to answer is how to efficiently choose the positions for the initial points. Although we can add a lot of points to cover all the existing points and discard unimportant ones after optimization, we still want reduce the number of initial points to save computational cost. One simple method is to randomly sub-sample a number of original points from the object. In this paper we propose a more efficient way to generate initial points as choosing the positions of critical points of the target. Critical points are those which finally contribute to the global feature vector after the max pooling operation in PointNet. This means that critical points are at the important positions for object shape determination. Therefore, adversarial points around these positions are more likely to change the final prediction.

We use Hausdorff and Chamfer measurements as the perturbation metrics \mathcal{D} for this attack because they are more capable of measuring how unnoticeable the adversarial point clouds of different dimensionality are.

3D Manufacturable Adversarial Point Clusters

Studies have pointed out that small perturbation in digital data are difficult to be realized, or manufactured, and likely to lose adversarial effects in the physical world (Kurakin, Goodfellow, and Bengio 2016; Evtimov et al. 2017; Athalye and Sutskever 2017). These limitations reduce the impact of unnoticeable adversarial examples. Considering more and more point cloud data is collected from real-world objects via devices such as Lidar (Wang, Peethambaran, and Chen 2018), we are motivated to propose algorithms for

manufacturable adversarial point clusters which can be synthesized in the physical world. For this attack, we aim to generate a small number (1-3) of noticeable point clusters which can be manufactured via 3D printing, and attached to the original object to mount physical attacks. Since manufacturable clusters are noticeable by design, we discard perturbation metrics used for unnoticeable point cloud and introduce new ones as below.

Perturbation Metrics

The perturbation constraints for adversarial cluster generation aim to encourage the adversarial points to concentrate into a small number of clusters and therefore manufacturable. Here we introduce farthest distance and center loss as the clustering constraints.

Farthest Distance. If the farthest pair-wise point distance in a point set is controlled within a certain threshold, the points in this set are able to form a shaped cluster. Formally, we define farthest distance of a point set \mathcal{S} as:

$$\mathcal{D}_{far}(\mathcal{S}) = \max_{x, y \in \mathcal{S}} \|x - y\|_2 \quad (7)$$

Center Loss. Center loss (Wen et al. 2016) is a constraint encouraging points to move towards their geometric center, which is defined as follows:

$$\mathcal{D}_{ctr}(\mathcal{S}) = \frac{1}{\|\mathcal{S}\|_0} \sum_{x \in \mathcal{S}} \|x - c\|_2, c = \frac{1}{\|\mathcal{S}\|_0} \sum_{y \in \mathcal{S}} y \quad (8)$$

where c is the geometric center of the point set \mathcal{S} .

Number of Clusters Added. Similar to the number of points added in the unnoticeable adversarial point cloud generation, the number of clusters added also serves as an additional metric for attack performance, which is hard bounded to 1-3 in our experiments.

Generating Manufacturable Point Clusters

Since the perturbation metric has changed to $\mathcal{D} : \mathbb{R}^{n \times 3} \rightarrow \mathbb{R}$, we need to reformulate Equation 2 as follow:

$$\min f(x') + \lambda \sum_i \mathcal{D}(\mathcal{S}_i), i \in \{1, 2, \dots, m\} \quad (9)$$

where \mathcal{S}_i is the i^{th} adversarial point cluster, and m is number of adversarial clusters.

Note that here we do not constrain the distance between the adversarial clusters and the original object, since if clusters are not on the object surface, we can use “sticks” to connect them to the object. However, if one wants to generate adversarial clusters close to the object surface, it can be easily achieved by including additional Hausdorff or Chamfer distance in the perturbation metric function \mathcal{D} .

Generating adversarial clusters is a special case of adding adversarial point clouds, so we can adopt the *initialize-and-shift* method used in adding new points for unnoticeable adversarial point clouds here. However, the challenge is how to initialize the adversarial clusters.

The extremely large 3D search space makes random initialization infeasible. Firstly, the number of required initial points would increase dramatically and make it computationally infeasible. Secondly, despite of the imposed

perturbation constraints, scattered initial points are difficult to cluster via gradient-based optimization, since points are likely to get stuck in their vicinity caused by the ubiquity of local-minima.

We cannot only initialize points to object surface neither. In the previous task for crafting unnoticeable adversarial point clouds, we can take the positions of existing points as initialization because we have the prior that the added points should be close to the surface of objects. For adversarial cluster generation, however, we are allowed to add clusters anywhere in the 3D space. Initializing points only around the object surface reduces the ability of adversary and decreases the attack success rate, according to our observation.

To find effective ways to initialize cluster searching, we leverage the idea of vulnerable regions. For formatted data like 2D images, it is common to impose a L_1 constraint to encourage the sparsity of the perturbation vector. The region with large perturbation under a proper L_1 constraint is believed to be important for model decisions and thus vulnerable to adversarial attacks. However, the L_1 constraint is unsuitable for point cloud data when adding adversarial points because it is hard to define a L_1 norm for two point clouds with different sizes. Instead of resorting to the L_1 constraint, we take advantage of critical points again to effectively find potentially vulnerable regions for initialization. According to the concept of critical points, there are some important points which collectively determine the global features of the object shape. Then it is reasonable to initialize points to the regions where critical points can be clustered. Given a victim object and a target class t' , the attack process is as follows:

1. Obtain the critical points of the objects in *target* class.
2. Use the clustering algorithm DBSCAN (Ester et al. 1996) to cluster the selected critical points.
3. Choose points in the k largest clusters as the initial points, where k is a self-chosen parameter as well as a metric for attack performance evaluation.
4. Optimize over Equation 9 using gradient-based algorithms and find optimal cluster positions and shapes.

Note that DBSCAN algorithm groups points which are closely packed, or whose point density in the neighborhood exceeds a certain threshold, and marks the other points lying in low-density regions as outliers (Ester et al. 1996). Thus, we are able to filter out outlier points and get compact clusters via DBSCAN. It is also worth mentioning that, besides tuning the parameters of the DBSCAN algorithm, it is essential to determine the number of objects in target class where we collect critical points from as well as the number of critical points selected from each object. If we only choose one object, the critical points are unlikely to form good clusters since critical points of one object usually scatter on the object surface. If too many objects are selected, however, the critical points may only form a large cluster and fail to help identify vulnerable regions. The reasons for tuning the number of critical points selected are similar, only a moderate number of selected points results in good critical point clusters. However, such parameter tuning does not need to be

very accurate, and a large range of such parameters can result in good attack performance. Optimal parameters are not required because the attack pipeline is dominated by the optimization over Equation 9. We will provide detailed experimental setting in the next section.

Experimental Results

In this section, we implement the proposed algorithms for different attack tasks and conduct extensively evaluation on attack performance based on various metrics. Additionally, we explore the transferability of generated adversarial point clouds across different 3D learning models.

Dataset and 3D Models

We use the aligned benchmark ModelNet40 (Wu et al. 2015; Sedaghat et al. 2017) dataset for our experiments. The ModelNet40 dataset contains 12,311 CAD models from 40 most common object categories in the world. 9,843 objects are used for training and the other 2,468 for testing. As done by Qi et al., we uniformly sample 1,024 points from the surface of each object, and re-scale them into a unit ball. We use the same PointNet structure as proposed in (Qi et al. 2016) and train the model with all ModelNet40 training data to obtain our victim model. The ModelNet40 dataset is very imbalanced. For our attacks, we randomly select 25 test examples from each 10 largest classes, namely airplane, bed, bookshelf, bottle, chair, monitor, sofa, table, toilet and vase, to generate adversarial point clouds for. For each victim data record, we generate adversarial examples targeted on the rest 9 classes.

Unnoticeable Point Cloud Evaluation

We evaluate the attack performance for two different attack tasks: shifting existing points and adding new points in the unnoticeable attack setting.

Shifting Existing Points. We use L_2 distance as the perturbation constraint \mathcal{D} in Equation 2 and minimizes the objective loss to find the optimal perturbation. To obtain good attack performance, it is essential to choose an appropriate value for the weight λ , which controls the balance between minimizing adversarial loss and perturbation magnitude. If the λ is too small, the perturbation constraint is not strong enough and the perturbation would become too obvious. On the other hand, a λ that is too large would result in minimizing perturbation magnitude only and fail to attack. For all of our attacks, we perform 10-step binary search for the near-optimal λ . During the search, we record the smallest perturbation $\mathcal{D}(x, x')$ and its corresponding adversarial example x' , and finally output the most unnoticeable adversarial example.

We report the experiment results for three cases: *best case* for the most easily attacked (victim, target) class pair, *average case* for all attacking class pairs, and *worst case* for the most difficult pair. The success rate and mean perturbation loss for point shifting attacks are reported in the first two columns of Table 1. We can see we successfully attack all victims examples into all target classes. The perturbation

Table 1: Attack performance evaluation for unnoticeable adversarial point clouds

Case	Shifting Points (L_2 Norm)		Adding Points (\mathcal{D}_H)			Adding Points (\mathcal{D}_C)		
	mean loss	success rate	mean loss	#points added	success rate	mean loss	#points added	success rate
Best	0.0874	100%	0.0003	93	100%	3.1×10^{-5}	58	100%
Average	0.3032	100%	0.0105	88	100%	2.7×10^{-4}	51	100%
Worst	0.4674	100%	0.0210	99	100%	7.2×10^{-4}	49	100%

Table 2: Attack performance evaluation for manufacturable adversarial point clusters

Case	#Cluster 1			#Cluster 2			#Cluster 3		
	\mathcal{D}_{ctr}	\mathcal{D}_{far}	success rate	\mathcal{D}_{ctr}	\mathcal{D}_{far}	success rate	\mathcal{D}_{ctr}	\mathcal{D}_{far}	success rate
Best	0.0077	0.0213	100%	0.0074	0.0210	100%	0.0076	0.0218	100%
Average	0.1967	0.6034	84.2%	0.0818	0.2906	99.6%	0.0453	0.1557	99.9%
Worst	0.2563	1.547	84.0%	0.1895	0.9623	96.0%	0.1309	0.6031	96.0%

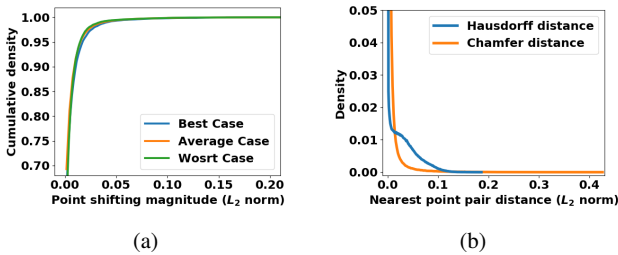


Figure 1: Distributions of point distances for unnoticeable adversarial point clouds. (a) CDF of point shifting distance; (b) Distributions for distance of nearest point pairs in point adding attack.

loss for this attack is relatively small, considering the perturbation vector contains 1,024 elements. To better understand the attack performance, we plot the distribution of perturbation magnitude (L_2 norm) for each point in Figure 1a. It is obvious that for all three cases, most points (80%) are barely shifted (less than 0.005), and the shifting distances for most shifted point are within 0.03, which is negligible comparing with the size of a unit ball.

We also provide adversarial point cloud visualization in the first row of Figure 2. We choose class “bottle” as our visualization victim because adversarial perturbation would become more obvious for a simple shape like a bottle. From the visualization, we can see the perturbation (the adversarial point cloud) is nearly indistinguishable.

Adding Adversarial Points. For adding adversarial points, we take Hausdorff and Chamfer measurements as perturbation metrics \mathcal{D} and optimize over Equation 2. We use two different distances separately and compare performance of these two constraints. To calculate the number of points added, we get the critical points of the newly generated adversarial point clouds, set T_{thre} to 0.01, and count over points moved further than it. The experiment results are shown in Table 1. First, both Hausdorff and Chamfer constraints result in attack success rate as 100%, proving the effectiveness of proposed *initialize-and-shift* algorithm. Secondly, we can

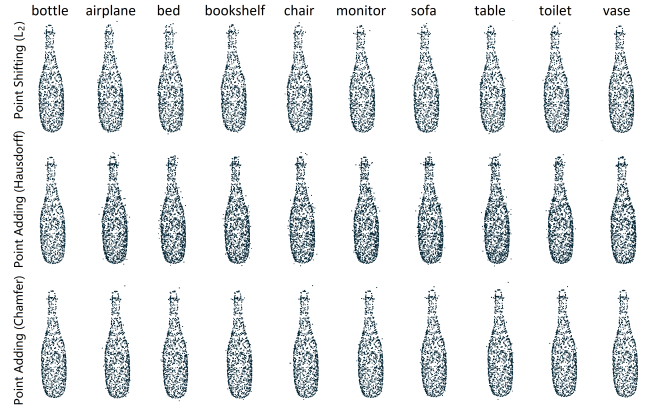


Figure 2: Visualization for unnoticeable adversarial point clouds

see great difference between the mean distance losses and number of points added. Since Hausdorff distance only controls the largest distance of all nearest point pairs while Chamfer measurement calculates the average distance, the loss value of Hausdorff is much larger than that of Chamfer and so does the number of points added. Another interesting finding is that the best case for Hausdorff constraint in terms of perturbation loss has more points added than the average case. This means Hausdorff distance does not explicitly constrain the number of points added.

To help further understand the characteristics of two distance constraints and explain why we include Hausdorff distance despite of its “poor” quantitative performance, we plot the distribution of distances from each point to the object surface in Figure 1b. As expected, the number, or percentage, of points with non-trivial distance for Hausdorff distance is larger than that of Chamfer measurement. However, it should be noticed that the largest distance of Hausdorff (0.18) is much smaller than that of Chamfer (0.42). This difference suggests that added points with Hausdorff constraint are likely to have fewer outliers, and thus less noticeable compared with those added based on Chamfer constraint.

The visualization of the adversarial bottle by adding

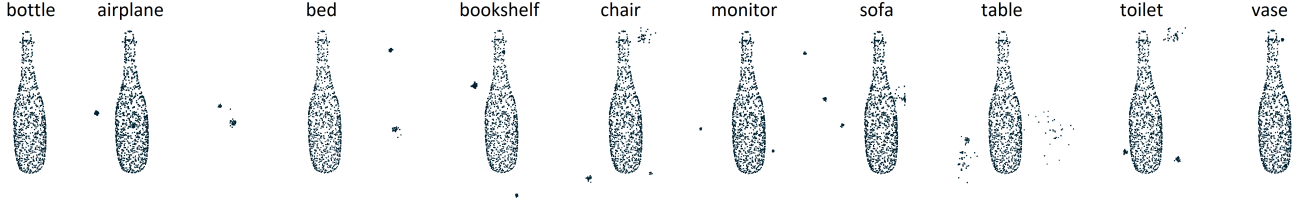


Figure 3: Visualization for adding 3 manufacturable adversarial point clusters.

points is shown in the second and third rows of Figure 2. From the figure, we can easily observe the different characteristics of different constraints (Hausdorff constraint results in more added points while Chamfer constraint leads to more obvious outliers), which is consistent with our quantitative results. In addition, due to the different properties of the two constraints, one can combine these two constraints and adjust the weights for the two perturbation metrics according to the specific attack goals.

Manufacturable Point Cluster Evaluation

To get initial clusters, we randomly select 8 different objects from the target class test set, and obtain 32 most important critical points for each selected object based on the number of global feature channels it contributes to. We then use DBSCAN algorithm to cluster these 32×8 critical points. After that, we retain k clusters of largest size and discard other small clusters and outliers. We vary k from 1 to 3 to see how the number of adversarial clusters affects the attack performance (success rate and distance loss). We take the farthest distance and center loss as the distance constraints in Equation 9. Due to the lack of space, we only report the results for adversarial clusters optimized based on the farthest distance in Table 2, but we still record both the farthest distance and center loss values of the same attack for comparison. The table shows that, as the number of adversarial clusters increases, the attack success rate is significantly improved and we are able to attack 99.9% examples when adding 3 adversarial clusters. Moreover, a larger number of added clusters also helps reduce the perturbation loss for each cluster. When we only add one cluster, the farthest distance of the cluster for average case is 0.6034, which is quite large considering the whole object fits in a unit ball. However, the farthest distance drops dramatically to 0.1557 when we are adding 3 clusters. Thus, it is reasonable to expect better attack performance if the adversary is able to add more than 3 clusters. One thing to be mentioned is that we report the (victim, target) pair with largest distance loss as the worst case. It is obvious that the lack of capacity (only able to add one cluster) can increase the attack difficulty.

Visualization for adding 3 adversarial clusters can be found in Figure 3. Several small clusters are clearly shown. For simplicity we only visualize the adversarial clusters and the original objects. It is possible to add several sticks to connect the adversarial points and the object surface. Since the surface area of a stick is negligible, it will not affect the adversarial behavior of these adversarial point clouds. We omit the results of adding artificial sticks to connect these

Table 3: Attack success rates of untargeted transfer attacks for point shifting, point adding, and 3 cluster manufacturable attack against PointNet++ and DGCNN.

	Shifting	Adding (D_H)	Adding (D_C)	3 Clusters
PointNet++	3.9%	8.9%	3.6%	7.1%
DGCNN	1.9%	6.8%	7.4%	14.0%

adversarial clusters with the original objects to appendix.

Transferability of Adversarial Point Clouds

Considering the transferability of 2D adversarial instances, here we aim to explore the transferability of the generated adversarial point clouds against other PointNet-like models. We feed our crafted adversarial point clouds to PointNet++ (Qi et al. 2017) and DGCNN (Wang et al. 2018) and find that these 3D adversarial examples actually hardly transfer as targeted attacks. Furthermore, we calculate the success rate for untargeted attack and the results are shown in Table 3. We can see the transferability for untargeted attack is also limited compared with 2D adversarial examples. Note that our proposed attack methods are general and can be applied to attack arbitrary 3D models, so the low transferability for 3D adversarial point clouds may be related with special properties of 3D models themselves. This is an intrinsic property since if the 3D models can control transferability of adversarial examples, it is possible to design black-box attacks against such adversarial instances. Therefore, applying PointNet-like structure to improve the robustness of traditional CNNs would be an interesting future work.

Conclusion

In this paper, we are the first to study the vulnerability of 3D learning models. We have proposed several attack methods for two types of attacks against irregularly formatted point cloud data: crafting *unnoticeable adversarial point clouds*, and generating *manufacturable adversarial point clusters*. We also propose 7 different perturbation metrics and extensively evaluate the performance of the proposed attack algorithms. Our extensive experimental results show that the proposed algorithms are able to find 3D adversarial point clouds with about 100% attack success rate given an acceptable perturbation budget. We hope this work is able to provide a baseline as well as a guideline for future 3D adversarial example research.

References

- [Athalye and Sutskever 2017] Athalye, A., and Sutskever, I. 2017. Synthesizing robust adversarial examples. *arXiv preprint arXiv:1707.07397*.
- [Carlini and Wagner 2016] Carlini, N., and Wagner, D. 2016. Defensive distillation is not robust to adversarial examples. *arXiv preprint arXiv:1607.04311*.
- [Carlini and Wagner 2017] Carlini, N., and Wagner, D. 2017. Towards evaluating the robustness of neural networks. In *Security and Privacy (SP), 2017 IEEE Symposium on*, 39–57. IEEE.
- [Carlini and Wagner 2018] Carlini, N., and Wagner, D. 2018. Audio adversarial examples: Targeted attacks on speech-to-text. *arXiv preprint arXiv:1801.01944*.
- [Das et al. 2018] Das, N.; Shanbhogue, M.; Chen, S.-T.; Chen, L.; Kounavis, M. E.; and Chau, D. H. 2018. Adagio: Interactive experimentation with adversarial attack and defense for audio. *arXiv preprint arXiv:1805.11852*.
- [Ester et al. 1996] Ester, M.; Kriegel, H.-P.; Sander, J.; Xu, X.; et al. 1996. A density-based algorithm for discovering clusters in large spatial databases with noise. In *Proceedings of the Second International Conference on Knowledge Discovery and Data Mining*, KDD’96, 226–231.
- [Evtimov et al. 2017] Evtimov, I.; Eykholt, K.; Fernandes, E.; Kohno, T.; Li, B.; Prakash, A.; Rahmati, A.; and Song, D. 2017. Robust physical-world attacks on deep learning models. *arXiv preprint arXiv:1707.08945* 1.
- [Fan, Su, and Guibas 2017] Fan, H.; Su, H.; and Guibas, L. J. 2017. A point set generation network for 3d object reconstruction from a single image. In *CVPR*, volume 2, 6.
- [Goodfellow, Shlens, and Szegedy 2014] Goodfellow, I.; Shlens, J.; and Szegedy, C. 2014. Explaining and harnessing adversarial examples. *arXiv preprint arXiv:1412.6572*.
- [Jia and Liang 2017] Jia, R., and Liang, P. 2017. Adversarial examples for evaluating reading comprehension systems. *arXiv preprint arXiv:1707.07328*.
- [Kurakin, Goodfellow, and Bengio 2016] Kurakin, A.; Goodfellow, I.; and Bengio, S. 2016. Adversarial examples in the physical world. *arXiv preprint arXiv:1607.02533*.
- [Meng and Chen 2017] Meng, D., and Chen, H. 2017. Magnet: a two-pronged defense against adversarial examples. In *Proceedings of the 2017 ACM SIGSAC Conference on Computer and Communications Security*, 135–147. ACM.
- [Moosavi-Dezfooli, Fawzi, and Frossard 2016] Moosavi-Dezfooli, S.-M.; Fawzi, A.; and Frossard, P. 2016. Deepfool: a simple and accurate method to fool deep neural networks. In *Proceedings of the IEEE Conference on Computer Vision and Pattern Recognition*, 2574–2582.
- [Papernot et al. 2016] Papernot, N.; McDaniel, P.; Jha, S.; Fredrikson, M.; Celik, Z. B.; and Swami, A. 2016. The limitations of deep learning in adversarial settings. In *Security and Privacy (EuroS&P), 2016 IEEE European Symposium on*, 372–387. IEEE.
- [Papernot et al. 2017] Papernot, N.; McDaniel, P.; Goodfellow, I.; Jha, S.; Celik, Z. B.; and Swami, A. 2017. Practical black-box attacks against machine learning. In *Proceedings of the 2017 ACM on Asia Conference on Computer and Communications Security*, 506–519. ACM.
- [Qi et al. 2016] Qi, C. R.; Su, H.; Mo, K.; and Guibas, L. J. 2016. Pointnet: Deep learning on point sets for 3d classification and segmentation. *arXiv preprint arXiv:1612.00593*.
- [Qi et al. 2017] Qi, C. R.; Yi, L.; Su, H.; and Guibas, L. J. 2017. Pointnet++: Deep hierarchical feature learning on point sets in a metric space. *arXiv preprint arXiv:1706.02413*.
- [Ranjan et al. 2017] Ranjan, R.; Sankaranarayanan, S.; Castillo, C. D.; and Chellappa, R. 2017. Improving network robustness against adversarial attacks with compact convolution. *arXiv preprint arXiv:1712.00699*.
- [Samangouei, Kabkab, and Chellappa 2018] Samangouei, P.; Kabkab, M.; and Chellappa, R. 2018. Defense-gan: Protecting classifiers against adversarial attacks using generative models. *arXiv preprint arXiv:1805.06605*.
- [Sedaghat et al. 2017] Sedaghat, N.; Zolfaghari, M.; Amiri, E.; and Brox, T. 2017. Orientation-boosted voxel nets for 3d object recognition. In *British Machine Vision Conference (BMVC)*.
- [Szegedy et al. 2013] Szegedy, C.; Zaremba, W.; Sutskever, I.; Bruna, J.; Erhan, D.; Goodfellow, I.; and Fergus, R. 2013. Intriguing properties of neural networks. *arXiv preprint arXiv:1312.6199*.
- [Wang et al. 2018] Wang, Y.; Sun, Y.; Liu, Z.; Sarma, S. E.; Bronstein, M. M.; and Solomon, J. M. 2018. Dynamic graph cnn for learning on point clouds. *arXiv preprint arXiv:1801.07829*.
- [Wang, Peethambaran, and Chen 2018] Wang, R.; Peethambaran, J.; and Chen, D. 2018. Lidar point clouds to 3-d urban models: a review. *IEEE Journal of Selected Topics in Applied Earth Observations and Remote Sensing* 11(2):606–627.
- [Wen et al. 2016] Wen, Y.; Zhang, K.; Li, Z.; and Qiao, Y. 2016. A discriminative feature learning approach for deep face recognition. In *European Conference on Computer Vision*, 499–515. Springer.
- [Wu et al. 2015] Wu, Z.; Song, S.; Khosla, A.; Yu, F.; Zhang, L.; Tang, X.; and Xiao, J. 2015. 3d shapenets: A deep representation for volumetric shapes. In *Proceedings of the IEEE conference on computer vision and pattern recognition*, 1912–1920.
- [Xiao et al. 2018a] Xiao, C.; Li, B.; Zhu, J.-Y.; He, W.; Liu, M.; and Song, D. 2018a. Generating adversarial examples with adversarial networks. *arXiv preprint arXiv:1801.02610*.
- [Xiao et al. 2018b] Xiao, C.; Zhu, J.-Y.; Li, B.; He, W.; Liu, M.; and Song, D. 2018b. Spatially transformed adversarial examples. *arXiv preprint arXiv:1801.02612*.
- [Xu, Evans, and Qi 2017] Xu, W.; Evans, D.; and Qi, Y. 2017. Feature squeezing: Detecting adversarial examples in deep neural networks. *arXiv preprint arXiv:1704.01155*.
- [Yan, Guo, and Zhang 2018] Yan, Z.; Guo, Y.; and Zhang, C.

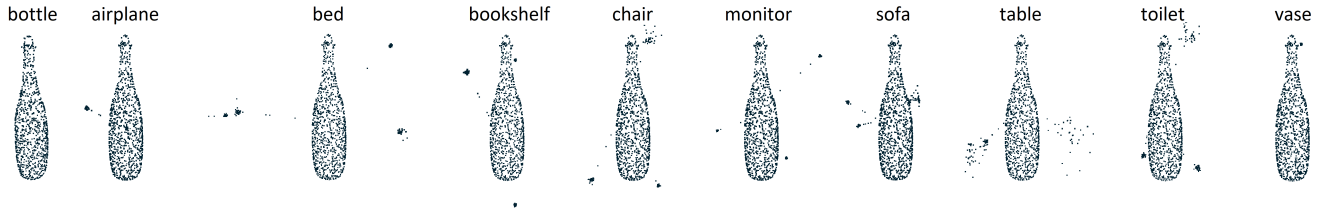


Figure 4: Visualization for adding 3 manufacturable adversarial point clusters by adding artificial sticks.

2018. Deepdefense: Training deep neural networks with improved robustness. *arXiv preprint arXiv:1803.00404*.

[Zermas, Izzat, and Papanikolopoulos 2017] Zermas, D.; Izzat, I.; and Papanikolopoulos, N. 2017. Fast segmentation of 3d point clouds: A paradigm on lidar data for autonomous vehicle applications. In *Robotics and Automation (ICRA), 2017 IEEE International Conference on*, 5067–5073. IEEE.

[Zhao, Dua, and Singh 2017] Zhao, Z.; Dua, D.; and Singh, S. 2017. Generating natural adversarial examples. *arXiv preprint arXiv:1710.11342*.

Case Study: Adding Artificial Sticks

To better understand the possibility to synthesize physical 3D perturbation, here we perform a case study by adding artificial sticks to connect our generated “adversarial point clusters” with the original object to fulfill this purpose.

Adding sticks. To simulate the point clouds with added sticks, we get the geometric center of each cluster, find the nearest point of the original object, and uniformly add points along the line drawn between cluster center and its corresponding nearest point.

Success Rate. We take the bottle used in previous visualization for our case study. We uniformly add 5 points for each stick and test whether the point clouds still succeed in targeted attack. The experiment is repeated multiple times for each target class and it retains high attack success rate for most classes. No matter what the target class is, we can always find successful adversarial examples.

Visualization. We provide similar visualization for successful adversarial examples in Figure 4. We can see clearly several sticks are added without neutralizing the adversarial effect. Note that during our optimization, we do not explicitly consider the existence of the sticks. How to improve the robustness of manufacturable adversarial point clusters against added sticks or other artificial objects may be an interesting future work.